Nonlinear Science and Intelligent Applications
https://www.acadlore.com/journals/NSIA

Nonlinear Electromechanical Dynamics of a DC Motor Driven by Fractional-Order Hindmarsh–Rose Neuronal Oscillations: Theory and Experiment

Thepi Siewe Raoul[1*], Goune Chengui Géraud Roussel[2], Endele Paul Patrick[3], Edima-Durant Hélène Carole[3,4], Atangana Jacques[1]

[1] Department of Apply Physics, Faculty of Science, University of Ebolowa, 9000 Ebolowa, Cameroon
[2] Department of Electrical Engineering, University of Dschang, 3060 Bandjoun, Cameroon
[3] Department of Biology and Plant Physiology, Faculty of Science, University of Ebolowa, 9000 Ebolowa, Cameroon
[4] Department of Biotechnology and Pharmacognosy, Faculty of Science, University of Ebolowa, 9000 Ebolowa, Cameroon

[*] Correspondence: Thepi Siewe Raoul (thepiraoul@yahoo.com)

Received: 07-21-2025 **Revised:** 09-12-2025 **Accepted:** 09-25-2025

Citation: T. S. Raoul, G. C. G. Roussel, E. P. Patrick, E. D. H. Carole, and A. Jacques, "Nonlinear electromechanical dynamics of a DC motor driven by fractional-order Hindmarsh–Rose neuronal oscillations: Theory and experiment," *Nonlinear Sci. Intell. Appl.*, vol. 1, no. 1, pp. 40–47, 2025. https://doi.org/10.56578/nsia010104.

Abstract: Neuronal oscillations generated by nonlinear dynamical systems have attracted increasing attention for bio-inspired actuation and control applications. In this study, a direct electromechanical coupling between a direct current (DC) motor and neuronal signals produced by a fractional-order Hindmarsh–Rose oscillator (FOHRO) was investigated. The FOHRO was realized using an Arduino–Simulink interface and was employed as a signal-generation unit whose output voltage was used to drive a DC motor. The oscillator was treated as a nonlinear wave-shaping element capable of generating pulse-like and bursting neuronal patterns through appropriate variation of its fractional order and system parameters. The resulting electromechanical system (EMS) was modeled by consistently incorporating Newtonian rotational dynamics and electrical circuit laws. A total energy function was defined, and a scaling transformation was applied to derive an equivalent dimensionless dynamical model. Numerical simulations demonstrated that, when driven by FOHRO-generated neuronal signals, the DC motor exhibited angular velocity responses that preserve the temporal characteristics of the underlying neuronal oscillations, including spiking and bursting regimes. These findings were validated experimentally through real-time microcontroller implementation, confirming close qualitative agreement between simulation and hardware results. The proposed framework provides fundamental insights into the interaction between fractional-order neural oscillators and electromechanical actuators and suggests potential design principles for bio-inspired robotic joints and artificial articulations subjected to electrical stimulation. Such architectures may be particularly relevant for soft robotics, neuro-robotic interfaces, and adaptive actuation systems requiring rich dynamical responses derived from biologically inspired signal sources.

Keywords: Fractional-order Hindmarsh–Rose oscillator; Arduino–Simulink; Direct current motor; Neuronal signal; Robotic artificial articulation; Microcontroller

1 Introduction

In the biological domain, neural activity in the nervous system depends on the activation of neurons and their interactions with astrocytes [1–3], and muscle contraction can be controlled by calcium current [4, 5]. Neuronal function is mediated through electrical signals. If signal propagation and information exchange in the nervous system are broken, some neural diseases occur, resulting in abnormal or unsafe gait patterns [6, 7]. Neuronal electrical activity arises from the interaction between the cell membrane and ion channels, leading to transitions in membrane potential and changes in local electric field energy during the continuous diffusion and propagation of ions within neurons. External stimuli just speed up the mode selection by changing the gradient distribution of the electromagnetic field of the cell. The propagated electric pulses are affected by the calcium wave and concentration, and coordinated muscle activation governs the generation of appropriate gait patterns. Besides experimental approaches and detection techniques, theoretical models have been developed to analyze and quantify neural activity, which is helpful to predict mode transitions in electrical dynamics [8, 9].

Over recent decades, electromechanical system (EMS) have benefited from significant technological advances and widespread development. These systems have been applied to different domains like bio-inspiration, biomimetic engineering, robotics, and the monitoring of the properties of individual cells [10–13]. EMSs are usually used as actuators to induce motion in mechanical devices, as well as in sensors to detect physical quantities such as acceleration, pressure, temperature, and so on [10–12]. Many studies have been conducted in the EMS domain. Among them, it can be noticed that EMSs subjected to alternating current excitation can exhibit complex dynamical behaviors [10, 11]. This complexity is a consequence of coupling or nonlinearities in the mechanical and transduction parts. It has been clearly demonstrated that nonlinear characteristics in the electrical/electronic parts can be introduced to obtain complex system responses. Simo Domguia et al. [10] proposed an EMS based on the implementation of the dynamical behavior of a capacitive microEMS powered by a Hindmarsh–Rose electronic oscillator and presented the rich behaviors, including pulse and bursting oscillations. These oscillations have been applied to most automation engineering, where the mechanical part is required to operate for a very short time and return to its resting state [10–12]. This can also give some hints in bioengineering of the robotic system as the electromechanics of the heart exhibits bursting phenomena [11].

Ma and Guo [12] demonstrated the possibility of integrating self-sustained electronic circuits to power a direct current (DC) motor. The primary objective was to investigate the resulting electromechanical dynamics of the system. The modeling approach adopted revealed that the electromechanical arm is described by an ordinary differential equation coupled to a set of three-dimensional fractional-order ordinary differential equations. The introduction of fractional-order dynamics enables a more realistic representation of the system. However, the implementation of the fractional-order operators using conventional electrical components remains a significant challenge. Therefore, microcontrollers have been used to implement fractional-order electrical signals. In this context, Arduino–Simulink has been utilized. Matrix Laboratory (MATLAB) is one of the suitable software used to solve different types of numerical problems like differential equations. Within the software, there are numerous toolboxes and functions already developed for data acquisition, identification, and control design. On the other hand, the Arduino–Simulink interface is an alternative low-cost interface used for real-time data acquisition and communication. Arduino is an open-source platform, with all the necessary tools and libraries available on its website (arduino.cc). The additional Arduino input/output (I/O) package needed to link both platforms (Simulink and Arduino) can be downloaded from the MathWorks File Exchange. In this study, a low-cost platform design using fractional-order Hindmarsh–Rose oscillator (FOHRO) was proposed to generate electrical signals for driving a DC motor under real-time conditions. This is fully motivated by the outstanding robustness and performance quality of the high computing power required for real-time implementation [13–15].

The aim of this study is to model and theoretically and experimentally investigate the behavior of a DC motor powered by an electronic implementation of the FOHRO generated using embedded technology, such as a microcontroller. The main objective is to reproduce the similar behavior of the FOHRO's neuronal signals and to examine their effectiveness in exciting the DC motor. The outline of the study is organized below. Section 1 provides the introduction. Section 2 presents the system modeling and discusses the theoretical and experimental results associated with the DC motor powered by FOHRO-based neuronal signals produced by a microcontroller. Section 3 presents the conclusions.

2 System Modeling

Figure 1 presents the protocol for the real signal implementation through MATLAB and Arduino.

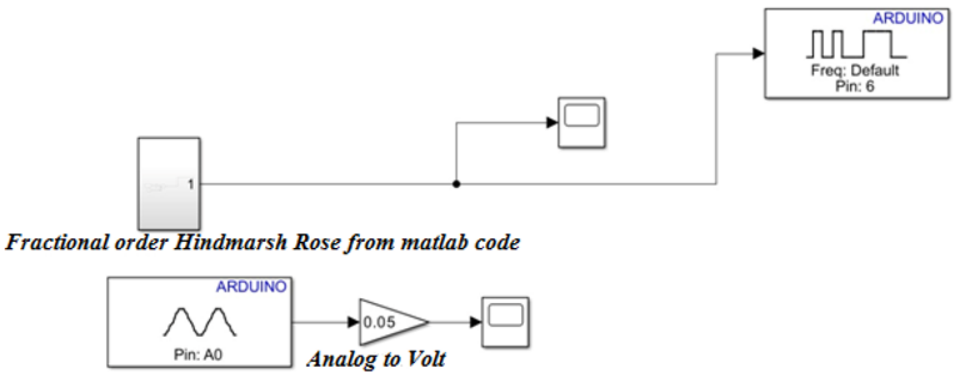

Figure 1. Presentation of the Matrix Laboratory (MATLAB)–Simulink–Arduino setup

In the setup in Figure 1, data are generated in the MATLAB program and imported into Simulink using the appropriate support package. The computer is connected to the Arduino board via a cable, and a potentiometer is employed to vary the real analog signal, which is monitored using an oscilloscope. The computer is used to manage and execute the program inside the microcontroller. Figure 2 presents the experimental setup. After obtaining the signal $x(t)$ from the Arduino, it is adapted using the IRF540 modulator to obtain $Ve(t)$ to actuate the DC motor. The mechanical rotation of the DC motor powers the generator that reproduces automatically the same wave signal $Vs(t)$ as $Ve(t)$, analyzing the mechanical response of the DC motor.

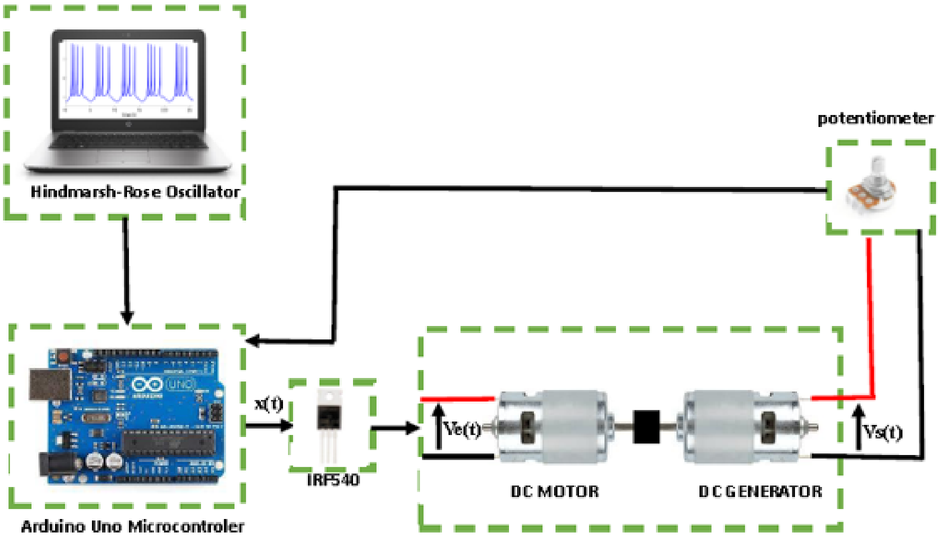

Figure 2. Schematic diagram of a direct current (DC) motor powered by neuronal signals of a fractional-order Hindmarsh–Rose oscillator (FOHRO) produced by a microcontroller

The FOHRO has been examined by several studies [13–15] and its rate equations are generally given by:

$$\begin{aligned} D^{q_1}x &= y - ax^2 + bx^3 - z + I_{ext} \\ D^{q_2}y &= c - dx^2 - y \\ D^{q_3}z &= r\left(s\left(x - x_0\right) - z\right) \end{aligned} \tag{1}$$

where, a, b, c, d, s are rare constants, and I_{ext} is the external input current (2.5 $< I_{ext} <$ 3.5).

System (1) is solved using the Grünwald–Letnikov approximation [16–21], by which the fractional-order operator can be expressed in the discrete form shown in System (2). For implementation on the microcontroller, the iteration equation used is given by:

$$\begin{aligned} x_i &= \left(y_{i-1} - ax_{i-1}^3 + bx_{i-1}^2 - zi - 1 + I_{ext}\right)h^{q_1} - \sum_{j=1}^{L}\omega_j^{q_1}x_{i-j} \\ y_i &= \left(c - dx_{i-1}^2 - y_{i-1}\right)h^{q_2} - \sum_{j=1}^{L}\omega_j^{q_2}y_{i-j} \\ z_i &= r\left(s\left(x_{i-1} - x_0\right) - z_{i-1}\right)h^{q_3} - \sum_{j=1}^{L}\omega_j^{q_3}z_{i-j} \end{aligned} \tag{2}$$

where, a = 1.0, b = 3.0, c = 1.0, d = 5.0, s = 4.0, r = 0.006, and x_0 = -1.6, L is the total computing size (L = 1000) [18].

According to Kirchhoff's voltage law, the governing equation of the electrical part of the DC motor in Figure 2 can be written as:

$$L_a\frac{di_e}{dt} = V_e - K_e\omega - R_a i_e \tag{3}$$

where, V_e and i_e are respectively the input voltage and current supply of the motor; K_e is the electromotive force constant; ω is the angular velocity of the motor; L_a is the armature inductance; and R_a is the armature resistance.

By applying Newton's second law for rotational motion, the mechanical dynamics are obtained as:

$$J\frac{d\omega}{dt} = K_t i_e - b_0\omega \tag{4}$$

where, K_t is the motor torque constant, and b_0 is the motor friction constant.

The motor-generator system is governed by the following set of equations:

$$\begin{aligned} L_a\frac{di_e}{dt} &= V_e - K_e\omega - R_a i_e \\ J\dot{\omega} &= K_t i_e - b_0\omega \\ L_a\frac{di_s}{dt} &= -V_s - K_e\omega - R_a i_s \\ J\dot{\omega} &= -K_t i_s - b_0\omega \end{aligned} \tag{5}$$

where, J is the inertia constant; V_s and i_s are respectively the output voltage and current delivers by the DC generator.

Figure 3 presents the equivalent electrical circuit that governs the proposed EMS in Figure 2.

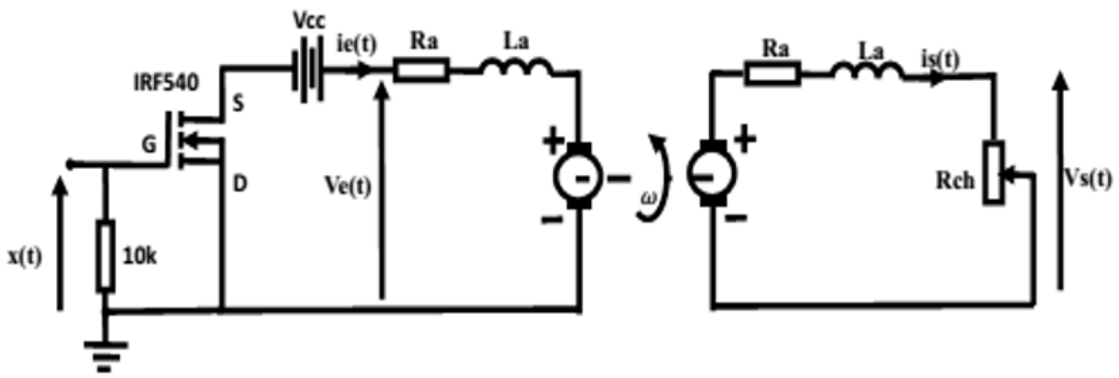

Figure 3. Equivalent circuit of the proposed electromechanical system (EMS)

From System (5), it appears that i_e = -i_s in the absence of a load V_s = $K_e\omega$. The signal applied to the metal oxide semiconductor field effect transistor (MOSFET). x is directly proportional to the input voltage of the motor V_e = kx since the MOSFET is in the commutation regime. The dimensional system of Eqs. (2)–(4) describes the proposed EMS in Figure 2. By combining these equations, the resulting equation is given as follows:

$$\begin{aligned} D^{q_1}x &= y - ax^2 + bx^3 - z + I_{ext} \\ D^{q_2}y &= c - dx^2 - y \\ D^{q_3}z &= r\left(s\left(x - x_0\right) - z\right) \\ \dot{x}_1 &= gx - a_1\omega - b_1\omega \\ \dot{\omega} &= a_2x_1 - b_2\omega \end{aligned} \tag{6}$$

With $x_1 = i_e$, $g = \frac{k}{L_a}$, $a_1 = \frac{K_e}{L_a}$, $b_1 = \frac{R_a}{L_a}$, $a_2 = \frac{K_t}{J}$, $b_2 = \frac{b_0}{J}$. For numerical simulations, the parameter values of the DC motor are g = 0.9, a_1 = 0.02, b_1 = 0.15, a_2 = 35, b_2 = 5. In this work, the same fractional-order values are considered like q_1 = q_2 = q_3 = q. By varying the fractional-order parameter q, System (6) can be solved numerically and the responses are plotted in Figure 4 below.

Figure 4 presents the numerical signals obtained using MATLAB from the solution of System (6).

By varying the value of the fractional-order parameter of the FOHRO, the system dynamics evolve from spikes to bursting oscillations, as shown in Figure 4. In the figure, the DC motor is excited by the neuronal signals of the FOHRO. The experimental setup of Figure 2 is presented in Figure 5.

This experimental setup in Figure 5 consists of the following components: (1) Arduino Uno board, (2) IRF 540 modulator, (3) stabilized voltage, (4) permanent-magnet KM34481D-5V DC motor, (5) DC generator, and (6) oscilloscope to visualize the electrical response through the DC generator. The motor used is a linear DC motor. The characteristics are given in Table 1.

Figure 6 presents the results obtained from the experimental setup in Figure 5 by considering the parameters in Table 1.

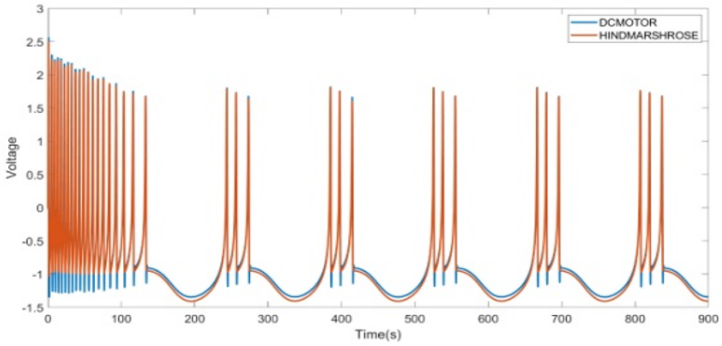

(a)

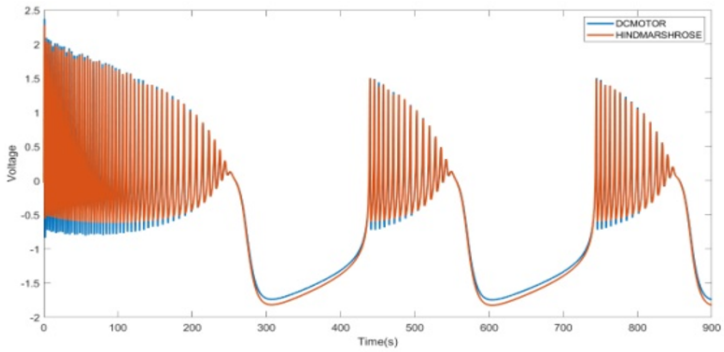

(b)

Figure 4. Numerical simulation of the fractional-order electrical part and the response of the direct current (DC) motor: (a) q = 1; (b) q = 0.9 with I_{ext} = 3

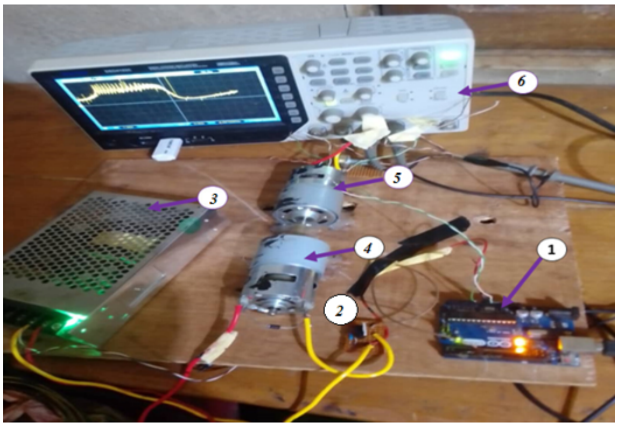

Figure 5. Experimental setup of the direct current (DC) motor powered by neuronal signals of the fractional-order Hindmarsh–Rose oscillator (FOHRO) implemented on a microcontroller

Table 1. Parameters of the KM34481D-5V direct current (DC) motor

Symbol	Value	Parameter
R_a	0.4 Ω	Armature resistance
L_a	2.7 mH	Armature inductance
b_0	2.2×10^{-3} N·m·s·rad^{-1}	Motor friction
K_t	1.5×10^{-2} N·m· A^{-1}	Motor torque
K_e	5.0×10^{-2} V·s·rad^{-1}	Electromotive
J	2.0×10^{-4} kg·m^2	Inertia constant

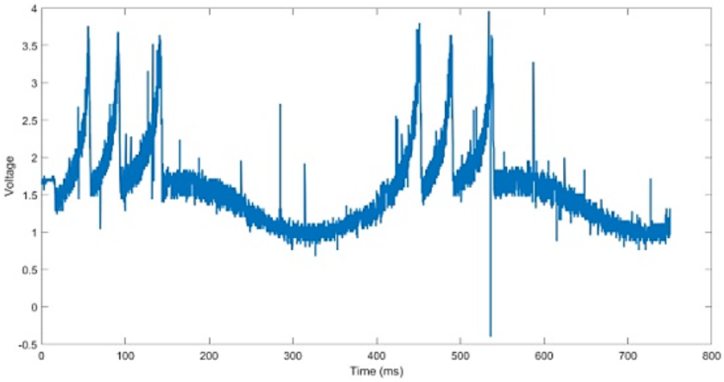

(a)

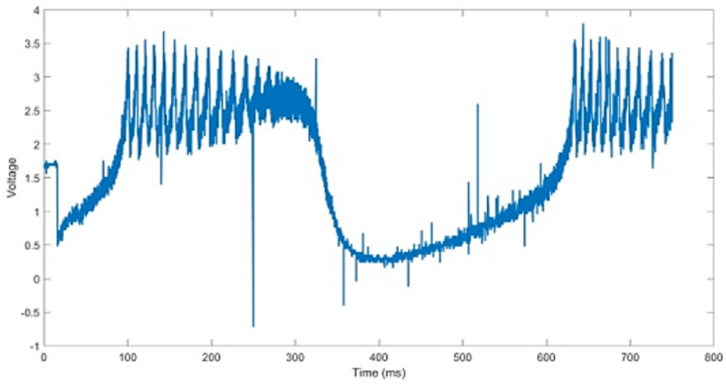

(b)

Figure 6. Experimental responses of the direct current (DC) motor for: (a) q = 1; (b) q = 0.9 with I_{ext} = 3

A qualitative comparison between Figure 4 and Figure 6 displays similar wave signals. However, the period and amplitude of the pulse oscillations are different. In terms of the oscillation period, the numerical response in Figure 4 exhibits a higher number of pulses compared to the experimental response in Figure 6. As for the amplitude, Figure 4 shows lower amplitudes compared with Figure 6. Since the DC motor is linear, nonlinearities occurring in the system cannot explain the differences. But possible explanations of this response of the system include the adaptation of the IRF540 modulator, the use of the voltage stabilizer, and the generator used to deliver voltage motion.

3 Conclusion

In this study, a DC motor powered by a FOHRO, acting as a model of neuron activity, was studied theoretically and experimentally. The rate equations of the proposed EMS were derived using Newtonian dynamics and electrical circuit laws. When the DC motor was excited by neuronal signals of the FOHRO, the transitions from spiking to bursting oscillations occurred by varying the values of the fractional-order parameter. The FOHRO was found to efficiently impose its bursting oscillations on the DC motor over a range of stable inertia coefficients. The qualitative agreement between numerical simulations and experimental results confirmed that the proposed interface can be useful. It was found that the developed system could potentially be used in robotic modeling, electromechanical education, experimental testing, and the development of low-cost laboratory kits. Moreover, the proposed approach may be extended to several fields. For instance, in artificial intelligence, robotics, and bio-mimetic engineering, the device and its dynamic responses could be used in applications requiring bio-inspired actuators capable of pulse-like actuation and robotic articulation driven by the mechanical response of a DC motor. In the bioengineering domain and bio-inspired applications, this study also offers insights into the design of neuron-activated prosthetic devices and other neuromorphic actuation systems, as well as potential applications in specialized defense and industrial technologies.

Author Contributions

Conceptualization, T.S.R.; methodology, T.S.R. and G.C.G.R.; software, T.S.R.; validation, T.S.R. and G.C.G.R.; formal analysis, T.S.R., G.C.G.R., and E.P.P.; investigation, T.S.R.; writing—original draft preparation, T.S.R.; visualization E.D.H.C. and A.J. ; supervision, E.D.H.C. and A.J. All authors have read and agreed to the published version of the manuscript.

Data Availability

The data used to support the research findings are available from the corresponding author upon request.

Conflicts of Interest

The authors declare that they have no conflicts of interest.

References

[1] C. Durkee, P. Kofuji, M. Navarrete, and A. Araque, "Astrocyte and neuron cooperation in long-term depression," *Trends Neurosci.*, vol. 44, no. 10, pp. 837–848, 2021. https://doi.org/10.1016/j.tins.2021.07.004

[2] C. G. Schipke and H. Kettenmann, "Astrocyte responses to neuronal activity," *Glia*, vol. 47, no. 3, pp. 226–232, 2004. https://doi.org/10.1002/glia.20029

[3] S. Ben Achour and O. Pascual, "Astrocyte–Neuron communication: Functional consequences," *Neurochem. Res.*, vol. 37, pp. 2464–2473, 2012. https://doi.org/10.1007/s11064-012-0807-0

[4] M. J. Berridge, "Smooth muscle cell calcium activation mechanisms," *J. Physiol.*, vol. 586, no. 21, pp. 5047–5061, 2008. https://doi.org/10.1113/jphysiol.2008.160440

[5] D. M. Bers, "Calcium and cardiac rhythms: Physiological and path physiological," *Circ. Res.*, vol. 90, no. 1, pp. 14–17, 2002. https://doi.org/10.1161/res.90.1.14

[6] G. Ricci, L. Volpi, L. Pasquali, L. Petrozzi, and G. Siciliano, "Astrocyte–Neuron interactions in neurological disorders," *J. Biol. Phys.*, vol. 35, pp. 317–336, 2009. https://doi.org/10.1007/s10867-009-9157-9

[7] B. E. Flucher and P. Tuluc, "How and why are calcium currents curtailed in the skeletal muscle voltage-gated calcium channels," *J. Physiol.*, vol. 595, no. 5, pp. 1451–1463, 2016. https://doi.org/10.1113/JP273423

[8] D. M. Bers, "Calcium fluxes involved in control of cardiac myocyte contraction," *Circul. Res.*, vol. 87, no. 4, pp. 275–281, 2000. https://doi.org/10.1161/01.res.87.4.275

[9] D. M. Bers and E. Perez-Reyes, "Ca channels in cardiac myocytes: Structure and function in Ca influx and intracellular Ca release. Cardiovasc," *Circul. Res.*, vol. 42, no. 2, pp. 339–360, 1999. https://doi.org/10.1016/S0008-6363(99)00038-3

[10] U. Simo Domguia, L. T. Abobda, and P. Woafo, "Dynamical behavior of a capacitive microelectromechanical system powered by a Hindmarsh–Rose electronic oscillator," *J. Comput. Nonlinear Dyn.*, vol. 11, no. 5, p. 051006, 2016. https://doi.org/10.1115/1.4032276

[11] U. Simo Domguia, M. V. Tchakui, H. Simo, and P. Woafo, "Theoretical and experimental study of an electromechanical system actuated by a Brusselator electronic circuit simulator," *J. Vib. Acoust.*, vol. 139, no. 6, p. 061017, 2017. https://doi.org/10.1115/1.4037139

[12] J. Ma and Y. Guo, "Model approach of electromechanical arm interacted with neural circuit, a minireview," *Chaos Solitons and Fractals*, vol. 183, p. 114925, 2024. https://doi.org/10.1016/j.chaos.2024.114925

[13] H. A. F. Berkani, B. Keziz, M. Lashab, A. Djouambi, and A. Kerrouche, "Low-cost platform for real time data acquisition and fractional control with application to a DC motor," *Int. J. Power Electron. Drive Syst.*, vol. 14, no. 4, pp. 2072–2079, 2023.

[14] Z. A. S. A. Rahman, B. H. Jasim, Y. I. A. AI-Yasir, R. A. Abd-Alhameed, and B. N. Alhasnawi, "A new no equilibrium fractional order chaotic system, dynamical investigation, synchronization, and its digital implementation," *Inventions*, vol. 6, no. 3, p. 49, 2021. https://doi.org/10.3390/inventions6030049

[15] I. Masngut, G. N. P. Pratama, A. I. Cahyadi, S. Herdjunanto, and J. F. J. Pakpahan, "Design of fractional-order proportional-integral-derivative controller: Hardware realization," in *2018 International Conference on Information and Communications Technology (ICOIACT)*, Yogyakarta, Indonesia, 2018, pp. 656–660. https://doi.org/10.1109/ICOIACT.2018.8350813

[16] J. L. Hindmarsh and R. M. Rose, "A model of neuronal bursting using three coupled first order differential equations," *Proc. Biol. Sci.*, vol. 221, no. 1222, pp. 87–102, 1984. https://doi.org/10.1098/rspb.1984.0024

[17] M. Łepek and F. Piotr, "Spatial evolution of hindmarsh–Rose neural network with time delays," *Nonlinear Dyn.*, vol. 92, pp. 751–761, 2018. https://doi.org/10.1007/s11071-018-4088-2

[18] D. Jun, Z. Guang-jun, X. Yong, Y. Hong, and W. Jue, "Dynamic behavior analysis of fractional-order hindmarsh–Rose neuronal model," *Cogn. Neurodyn.*, vol. 8, pp. 167–175, 2014. https://doi.org/10.1007/S11571-013-9273-X

[19] G. Adomian, "A review of the decomposition method and some recent results for nonlinear equations," *Math. Comput. Model.*, vol. 13, no. 7, pp. 17–43, 1990. https://doi.org/10.1016/0895-7177(90)90125-7

[20] W. M. Ahmad and J. C. Sprott, "Chaos in fractional-order autonomous nonlinear systems," *Chaos Solitons and Fractals*, vol. 16, no. 2, pp. 339–351, 2003. https://doi.org/10.1016/S0960-0779(02)00438-1

[21] E. Ahmed, A. M. A. El-Sayed, and H. A. A. El-Saka, “Equilibrium points, stability and numerical solutions of fractional-order predator–prey and rabies models,” *J. Math. Anal. Appl.*, vol. 325, no. 1, pp. 542–553, 2007. https://doi.org/10.1016/j.jmaa.2006.01.087